Tremor asperities in the transition zone control evolution of slow earthquakes

Abhijit Ghosh,[1] John E. Vidale,[2] and Kenneth C. Creager[2]

[1]   Slow earthquakes, characterized by slow slip and associated seismic radiation called non-volcanic tremor, have been observed in major subduction zones worldwide. They constitute an important mode of stress release for the fault's transition zone, which lies directly downdip of the locked segment, the nucleation zone of large damaging earthquakes. However, the depth of tremor in Cascadia, and the factors governing tremor generation and rupture propagation during slow quakes remain enigmatic. Here, we develop a novel multibeam-backprojection (MBBP) method to detect and locate tremor using multiple mini seismic arrays. We apply this technique to image tremor activity during an entire ETS-cycle including a large episodic tremor and slip (ETS) event in Cascadia with unprecedented resolution. Our results suggest that the majority of the tremor is occurring near the plate interface. We observe strongly heterogeneous tremor distribution with patches in the transition zone that experience repeated tremor episodes and produce most of the tremor. The patches, tens of kilometers in dimension, behave like asperities on the fault plane. During the large ETS event, rupture propagation velocity varies at least by a factor of five, and seems to be modulated by these tremor asperities. These observations support a model in which the transition zone is heterogeneous and consists of patches of asperities with surrounding regions slipping aseismically. The asperities fail quasi-periodically releasing stress and appear to regulate rupture propagation and tremor generation during slow earthquakes. This study presents new observations revealing the tectonic characteristics of the transition zone controlling the generation and evolution of slow earthquakes.

1.   Introduction

[2] Since the discovery of slow earthquakes about a decade ago, it has become clear that they play a major role in the plate boundary dynamics. For a long time, regular earthquakes were believed to be the main mode of unsteady stress release for faults. Recent studies on slow quakes [*Obara*, 2002; *Rogers and Dragert*, 2003] forced earth scientists to rethink this paradigm. Slow quake as large as Mw 6.8 has been reported [*Szeliga et al.*, 2008], but unlike their regular counterpart, they occur in the transition zone, directly downdip of the locked zone where the majority of

the regular earthquakes nucleate. Non-volcanic tremor is the seismic signature of slow earthquakes. Tremor has been observed to be stimulated by low stresses – tiny tidal stress [*Rubinstein et al.*, 2008] and dynamic stress [*Ghosh et al.*, 2009a] from the passage of teleseismic waves. Large regular megathrust earthquakes are often observed to break patches of asperities [*Lay et al.*, 1982] on the locked part of the fault plane as rupture propagates along-strike at near-shear wave velocity. How large slow earthquakes operate in the transition zone, however, remains enigmatic. Large slow quakes show along-strike rupture propagation in the form of tremor migration mimicking regular fast earthquakes, except that they are 4 orders of magnitude slower (~10 km/day [*Ghosh et al.*, 2009b, 2010a; *Obara*, 2010]) and occur in the transition zone.

[3] Asperities are considered relatively stronger patches on the fault plane. They are broken during unsteady fault movement and radiate bursts of seismic energy. Asperities may be produced by the topography, structure, compositional and/or rheological heterogeneity of the fault surface. They also appear to play a major role in determining the seismic behavior of the fault segment that is slipping mostly aseismically [*Rubin et al.*, 1999], with only intermittent microearthquakes. To what
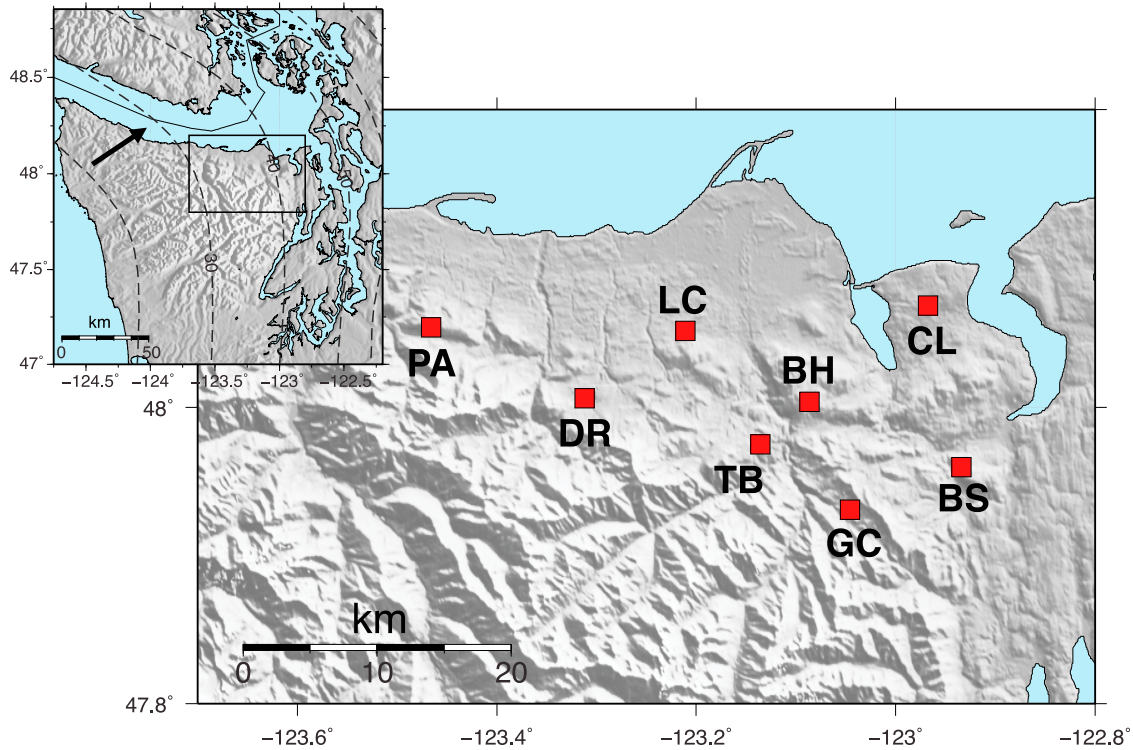
[1]Department of Earth Sciences, University of California, Riverside, California, USA.
[2]Department of Earth and Space Sciences, University of Washington, Seattle, Washington, USA.

Corresponding author: A. Ghosh, Department of Earth Sciences, University of California, Riverside, CA 92521, USA. (aghosh.earth@gmail.com)

Figure 1. Map showing the location of the 8 arrays (red squares) used in this study. Two letters corresponding to each array are the abbreviated names of the arrays. Inset shows the study area with the box marking the area covered in the main map. The arrow indicates the convergence direction of the Cascadia subduction zone. Dashed contour lines represent a model of the depth of the plate interface [*McCrory et al.*, 2006].

extent the evolution of slow earthquakes (tremor episodes) is affected by the asperities, if at all, is unknown.

[4] The details of the spatiotemporal distribution of tremor activity remain blurry due to the difficulty in detecting and locating tremor. Existing models are based solely on discrete slow seismic events [*Ito et al.*, 2007; *Shelly*, 2010] often detectable during tremor episodes (low frequency earthquakes, very low frequency earthquakes), and provide a good phenomenological description [*Obara*, 2011]. For rupture propagation during slow quakes, stress transfer [*Ghosh et al.*, 2010a] and diffusion [*Ide*, 2010] have been suggested as driving mechanisms. How transition zones regulate the overall seismic radiation and rupture propagation during large slow quakes, however, is not clear. Moreover, whether tremor in Cascadia occurs near the plate interface, or distributed over a wide depth range is still unresolved, and remains a matter of debate [*Kao et al.*, 2005; *Shelly et al.*, 2006].

2. Data and Seismic Arrays

[5] We installed 8 small-aperture seismic arrays, henceforth called the Array of Arrays (AofA), in the Olympic Peninsula, northern Washington, over the migration path of tremor during ETS events (Figure 1). Each array was armed with 10–20 3-component sensors, and augmented by 10 additional single-component vertical-channel sensors during ETS event. The instrument pool we used mainly consisted of L-28 3-component sensors and vertical-channel geophones

with a natural frequency of 4.5 Hz. We also used a few CMG-40T and broadband sensors. We recorded continuous ground velocity data at 50 samples per second, which meant that we had reliably recorded energy up to at least 20 Hz. Each array had an aperture between 1 and 2 km, and was designed to capture tremor activity. In order to conserve power to record an ETS event, five arrays were turned off for 2 to 4 months in different time periods such that at least 5 arrays were operating at all times. The sites of the arrays were carefully chosen to maximize our ability to image slow earthquakes by detecting and locating tremor activity using array techniques.

3. Multibeam-Backprojection Algorithm

[6] We developed a multibeam-backprojection (MBBP) technique (Figure 2) to detect and locate tremor. In this method, beam forming was performed in the frequency domain at each array to determine the slowness vectors [*Gerstoft and Tanimoto*, 2007; *Johnson and Dudgeon*, 1993]. We used vertical channel, 5–9 Hz energy with 1-min sliding independent (no overlap) time windows. At each window, slowness corrections were applied based on the array calibration using regular earthquakes cataloged by the Pacific Northwest Seismic Network. Then the arrays showing steep energy were selected eliminating the arrays dominated by shallow coherent noise. To remove local impulsive earthquakes, arrays only with stable slownesses over a five-minute time window were considered. After that, the arrays
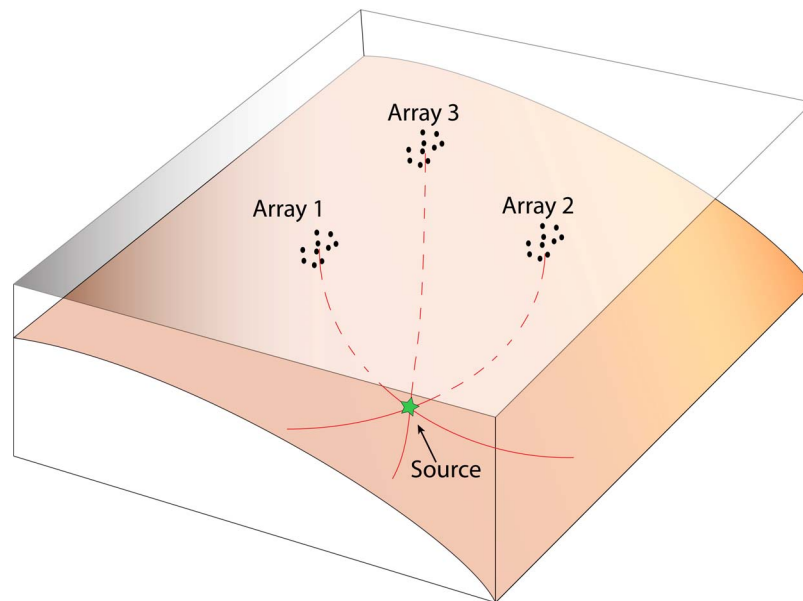
Figure 2. Schematic diagram showing basic idea behind multibeam-backprojection (MBBP) algorithm.

pointing to the same general area were selected. Finally, the slownesses from the arrays that passed all the criteria were backprojected in 3-D space to locate tremor source. In each time window, at least 3 arrays were required to determine a location. More accurate locations are obtained by requiring the arrays to point to the same general direction in the 3-D space. We used a 1-D *P*-wave velocity model [*Crosson*, 1976] for backprojection. Only stable locations were cataloged and used for this study. This process produced a tremor catalog with tremor location every 1-min, whenever detected. 14216 tremor locations obtained using MBBP method are used to make Figure 3. About 57% of the tremor locations plotted represent activity during the ETS event in August 2010. As shown in the next section, this new technique detected longer duration of tremor activity and located tremor with much higher resolution compared to a conventional envelope cross-correlation (ECC) method [*Wech and Creager*, 2008]. To achieve improved resolution at depth, centroid tremor locations of every half-an-hour were determined from the tremor catalog with 1-min time window. Time windows with fifty percent overlap were used and only stable centroid locations were kept. MBBP technique was able to determine tremor depth over half-an-hour time-scale, and produced a tremor catalog with reasonably constrained tremor depth. 290 locations with depth resolution were obtained using this technique. Average formal uncertainty in tremor locations is estimated using a bootstrap method. It is found to be 3 km in horizontal and 4 km in vertical direction. MBBP method was applied to ∼15.5 months of seismic data recorded by AofA, from mid-June 2009 to September 2010. It captured a full ETS-cycle, which included the ETS event in August 2010 and a complete inter-ETS time period, ∼14 months preceding the ETS event.

4. Observations and Discussions

[7] The tremor catalog created using the MBBP method provided an account of tremor activity in this region in great detail revealing several new and interesting features. Overall, we detected about 650 h of tremor spanning the area along-dip between the surface projection of 30 and 40 km depth contours of a model plate interface [*Audet et al.*, 2010] (Figure 3 and 4).

4.1. Tremor Depth

[8] The majority of the tremor was located near the model plate interface and aligned roughly parallel to it, suggesting that tremor in Cascadia is closely associated with the plate interface (Figure 4). Tremor locations formed a dipping layer sub-parallel to the layer of regular earthquakes. Overall, ordinary earthquakes seem to occur a few kms below the layer of the highest tremor concentration at depth. The dipping tremor layer in the cross section, however, stopped at about 40 km depth, while the layer of regular earthquakes continued deeper with the oceanic plate (Figure 4). This scenario is similar to what had been observed in southwest Japan, where sub-parallel layers of low-frequency earthquakes (LFE) and regular seismicity were separated by 5–8 km in depth [*Shelly et al.*, 2006]. The similarity of the depth distribution of tremor and regular events, spectral characteristics of tremor [*Shelly et al.*, 2007], combined with their association with slow slip in both Cascadia and Japan [*Ito et al.*, 2007; *Rogers and Dragert*, 2003] suggest that tremor in these two subduction zones are governed by the same physical process. As tremor in Japan is shown to be a result of shear slip on fault plane [*Shelly et al.*, 2006], it is likely that tremor in Cascadia occurring near the plate interface is a result of shear slip on the subduction fault.

4.2. Repeating Patches

[9] We found that spatial tremor distribution was far from uniform. Overall, northern part of the area imaged by the arrays showed more duration of tremor activity relative to the southern part. Tremor zone appeared to be heterogeneous with several distinct patches producing the majority of the tremor (Figure 3), supporting the observation made using
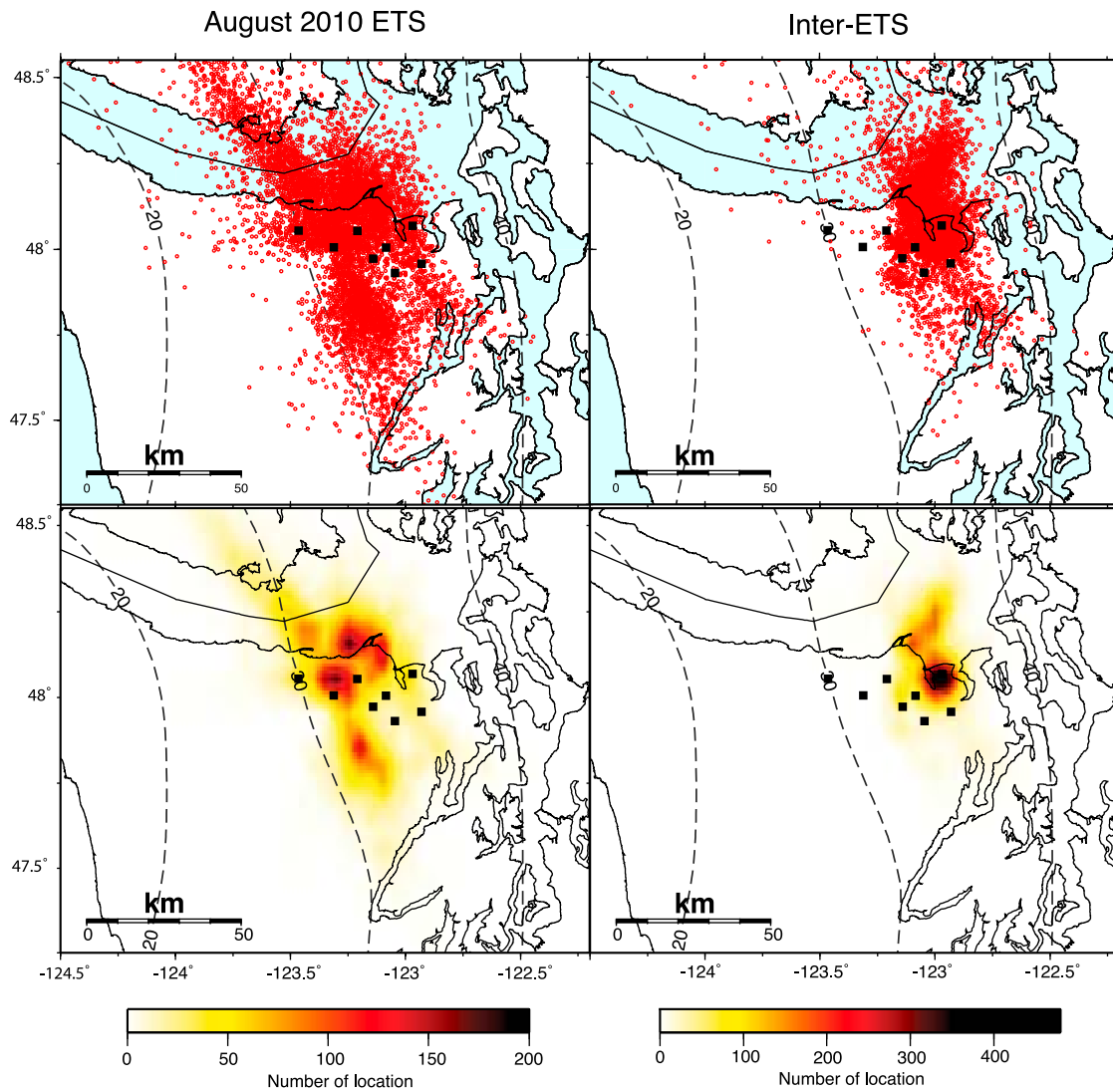
Figure 3. (top) Tremor location during the ETS, and inter-ETS time periods. (bottom) Tremor density. There are 8168 locations used for the ETS time period, and 6048 for inter-ETS. Note the heterogeneous and patchy nature of the spatial distribution of the tremor location. Black squares are the mini seismic arrays. Dashed contour lines represent a model of the depth of the plate interface [*Audet et al.*, 2010]. To make the tremor density plots, tremor locations are binned every 0.05°. The numbers in the bins are interpolated to make smoother plots.

a solo mini seismic array [*Ghosh et al.*, 2009b]. For the purpose of the present study, patches are referred to areas producing majority of the tremor and/or experiencing repeated tremor episodes. Based on the tremor activity, there were broadly two groups of patches: downdip and updip patches. As the names suggest, they occupied downdip and updip parts of the tremor zone. A bimodal distribution of tremor along-dip of the tremor zone in southwest Japan had also been reported [*Obara et al.*, 2010]. In the updip side of the tremor zone, we mapped 3–4 patches that showed concentrated tremor activity that were produced only by the activity during the ETS event (Figure 3). Among them, 2–3 patches were in north and one in south with a relatively inactive zone in between the southern and northern patches. In contrast, the downdip side of the tremor zone in this region was characterized by three patches, which produced

repeated tremor episodes in each patch during the inter-ETS time period (Figure 3 and 5, see Animation S1 in the auxiliary material).[1] Each of the downdip repeating patches experienced 10 to 15 tremor episodes, 38 in total, which lasted from 2 h to 6 days, and were equivalent to Mw 4.5–5.7 slow earthquakes, based on the observed linear moment-duration scaling of slow events [*Ide et al.*, 2007]. Relatively larger inter-ETS episodes showing coherent rupture propagation were the results of successive failure of multiple downdip patches. The downdip patches imaged in this study were closely spaced without clear gaps in between. Interestingly, activities of the repeating patches increased prior to the ETS and the largest inter-ETS event in March 2010.
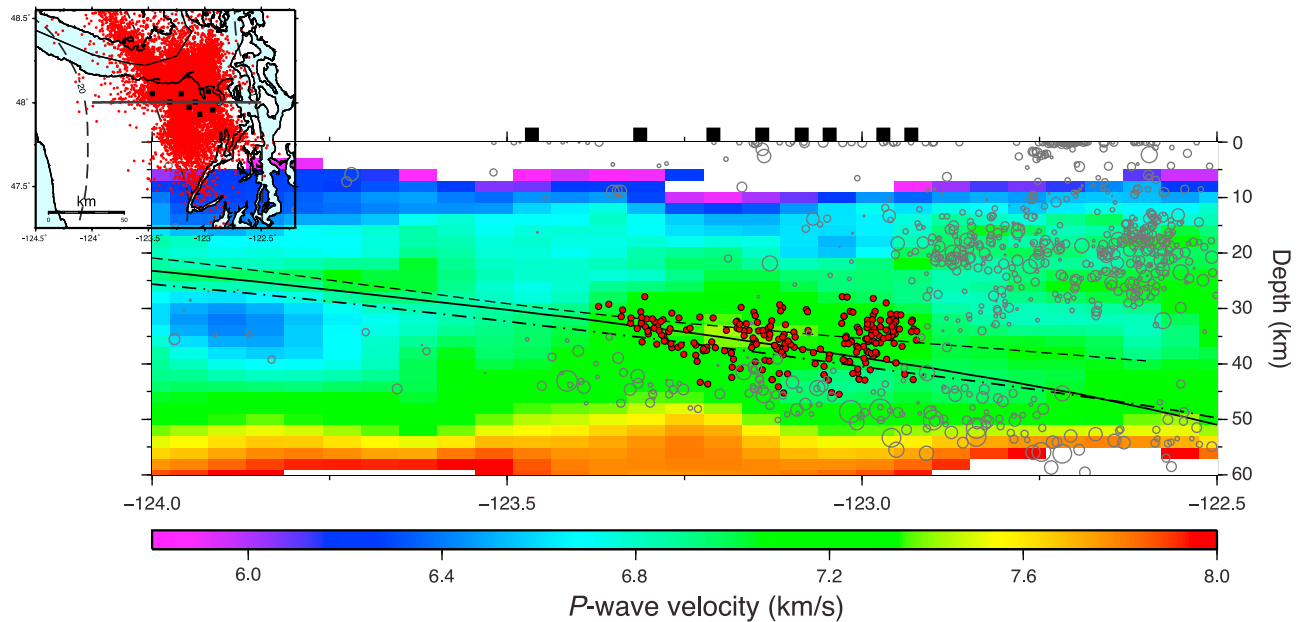
Figure 4. Cross-section at the bottom shows tremor location (red circles), regular earthquakes (gray open circles), three different models of the plate interface, and P wave velocity model. Inset map shows all tremor location with the EW line along which the cross-section is made. Tremor locations are determined using the MBBP algorithm. Earthquake locations are taken from catalog made by the Pacific Northwest Seismic Network. Circles size is scaled with earthquake magnitude. Three models of the plate interface are shown by dashed [*Audet et al.*, 2010], dashed-and-dot [*McCrory et al.*, 2006], and solid [*Preston et al.*, 2003] black lines. In the cross-section, events within 0.15° north and south of the EW-line are selected. 230 tremor locations are plotted. Background colors show P wave velocity model derived by [*Preston et al.*, 2003].

Many of these inter-ETS episodes remained undetected by a conventional ECC method of tremor detection and location [*Wech and Creager*, 2008]. It is important to note that there are areas that are clearly visible by the AofA and well within the tremor zone, but show little to no tremor activity (Figure 3) indicating that the heterogeneous tremor distribution is not an artifact caused by AofA geometry.

4.3. Rupture Propagation

[10] An important characteristic of earthquakes is their dynamic rupture propagation. We used migration of tremor, and by inference, seismic slip, to image several intriguing aspects of rupture propagation during slow earthquakes. One of the most prominent and widely observed features of large slow quakes is their along-strike rupture propagation at an approximately uniform velocity of ∼10 km/day [e.g., *Ghosh et al.*, 2009b, 2010a; *Obara*, 2010]. Here, we resolved remarkable variation in rupture propagation velocity, by at least a factor of 5, during the August 2010 ETS event (Figure 6). At the beginning of the event, rupture propagated north for 5 days or so at an average velocity of 4 km/day and broke the southern up- and downdip patches. On 16th August, rupture propagation velocity shot up to ∼20 km/day, a factor of 5 increase in rupture velocity. This increased velocity was maintained for 1.5 days, as tremor was propagating through a relatively inactive area between updip southern and northern patches. Tremor activity remained updip during this time. Then the along-strike propagation was halted for a day or two as the slow quake started breaking the northern patches, both up- and downdip. During this

time, tremor showed up- and downdip migration observed over shorter time-scales (Figure 7c). From 20th August, rupture continued to propagate north again with an average velocity of ∼4 km/day. Overall, rupture propagated along-strike south to north with an average velocity of 7–8 km/day, but as described above, showed considerable variation in its pattern. In short, rupture propagation is slow in the patches and fast in region in between the patches.

[11] MBBP method resolved rupture propagation even during moderate-size inter-ETS episodes (Figure 8 and 9). The weeklong March 2010 episode was a particularly interesting example (Figure 8). A remarkable aspect of this event was that it appeared to break the northern and southern downdip patches simultaneously as rupture propagated from north and south to converge under the CL array when the central patch failed. Then it propagated updip for about a day followed by a daylong quiescence. Finally, it culminated with a burst of tremor, which lasted for a few hours at the updip edge of the inter-ETS tremor zone. In addition, we observed at least another episode that involved multiple patches, and showed along-strike rupture propagation. This episode occurred in November 2009, propagated southward breaking the northern and central patches (Figure 9). Throughout these episodes, the rupture velocity on average remained between 5 and 10 km/day, comparable to the slow along-strike rupture propagation of the ETS event. Such complexities in moderate-sized slow earthquakes has not been fully captured previously due to the lack of resolution of the conventional methods. Successive failure of multiple downdip patches appears to be responsible for
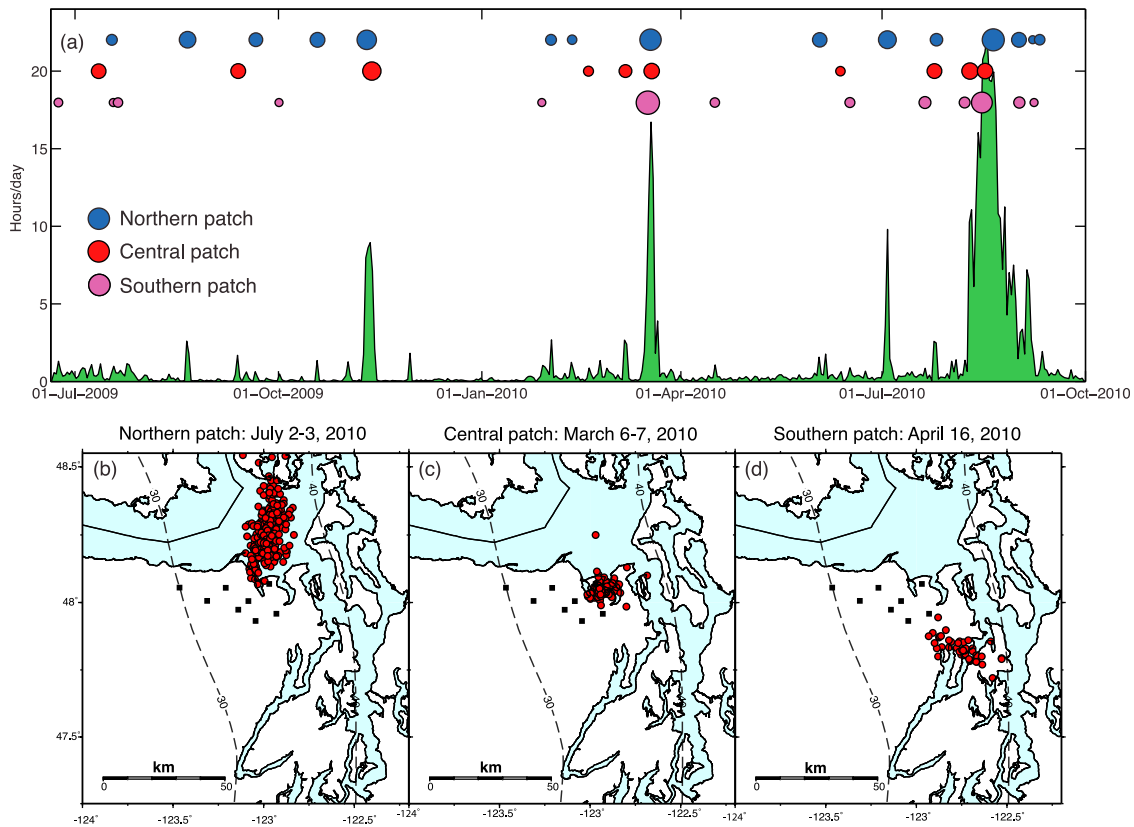
Figure 5. (a) Tremor activity detected by the MBBP algorithm during the 15.5 months studied here. Colored circles indicate timings and durations of the tremor episodes occurring repeatedly in three downdip patches. Circles are scaled by the duration (the largest 6 days, the smallest 2 h). (b–d) Examples of typical tremor episodes in each downdip patch. 218, 168, and 44 tremor locations are plotted respectively. Southern patch is by far the weakest one in terms of tremor activity.

generating smaller tremor episodes showing coherent rupture propagation.
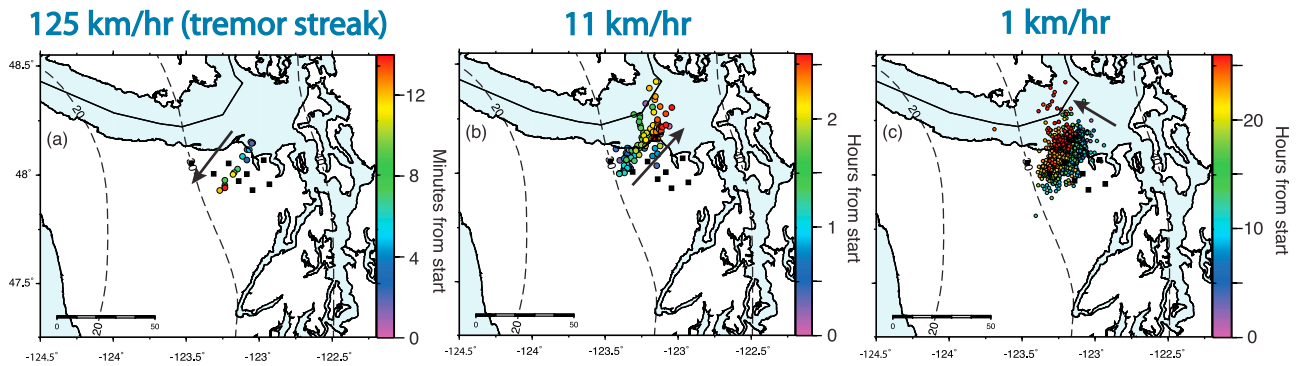
4.4. Different Flavors of Tremor Propagation

[12] Over short time-scales, from a few minutes to a day, tremor propagation showed a wide range of behaviors within the same general area (Figure 7). Rapid streaking of tremor at a velocity of ∼100 km/h and sub-parallel to the slip direction was the most dominant pattern, as had also been observed during the 2008 ETS event in this area [*Ghosh et al.*, 2010b]. In addition, we observed propagation velocities ranging from 11 km/h to 1 km/h in different directions. These velocities were much slower than the typical velocity of tremor streaks, and often much faster than the slow along-strike rupture
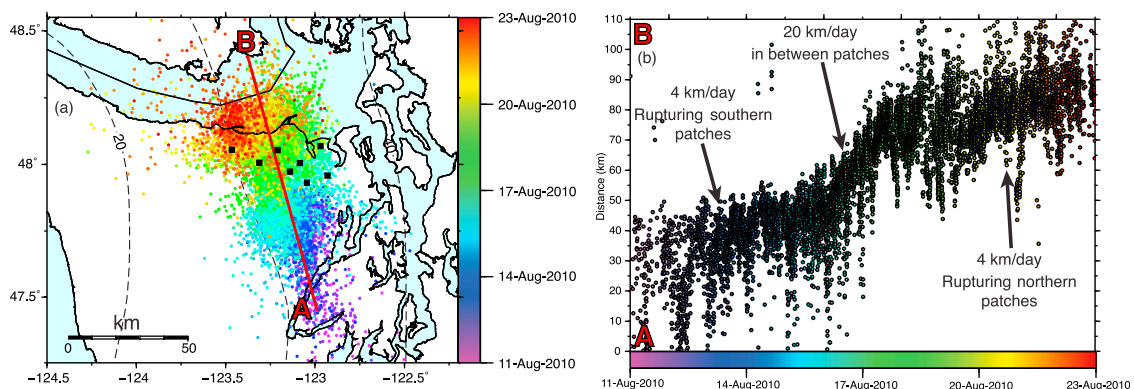
Figure 6. (a) Along-strike tremor migration during 2010 ETS event color-coded by time. Tremor migration is used as a proxy for rupture propagation. (b) Rupture propagation in a time-distance plot. Tremor locations are projected onto the NNW-SSE red line in Figure 6a.

Figure 7. Different flavors of tremor propagation over short time scales. Note the wide variation in propagation velocity and timescale. The timings of the migration events are as follows: (a) 8/17/2010 8:02:00–8:16:00, (b) 8/19/2010 2:11:00–4:47:00, (c) 8/17/2010 10:05:00–8/18/2010 12:56:00.

propagation, but overlapped with the range of velocities observed for rapid tremor reversals (7–17 km/h) [*Houston et al.*, 2011].

4.5. Model

[13] Regular fast earthquakes are thought to be a result of breaking asperities on faults [*Lay et al.*, 1982]. In the tremor zone, stationary downdip patches behave like asperities on the plate interface that are broken repeatedly producing tremor episodes, and by inference, slow slip events. Spatial stability of the downdip patches over multiple tremor episodes indicates that they might be caused by the rheological properties of the interface. During the ETS event, rupture slowly propagates along-strike breaking both up- and downdip patches and shows a factor-of-five variation in the propagation velocity. Rupture velocity is slower in the patches and faster in the region in between them. The

observations made in this study support a model of heterogeneous transition zone with patches of asperities (Figure 10). The asperities are the patches that can withstand relatively higher stress than the surrounding regions. The regions surrounding the asperities may experience relatively steady aseismic slip building up stress in the patches. The patches, on the other hand, slip quasi-periodically to release stress producing slow earthquakes and radiate seismic energy in the form of tremor. The episode becomes large when multiple patches are involved showing coherent rupture.

[14] In terms of its frictional characteristics, tremor zone is generally weaker than the locked zone updip. Tremor zone is spatially heterogeneous, as suggested by the observations presented here. So far, there is no evidence of heterogeneous stress drop for slow earthquakes. In fact, slow earthquakes are modeled as constant low stress-drop events [*Ide et al.*, 2007]. Therefore, the patches with relatively high stress
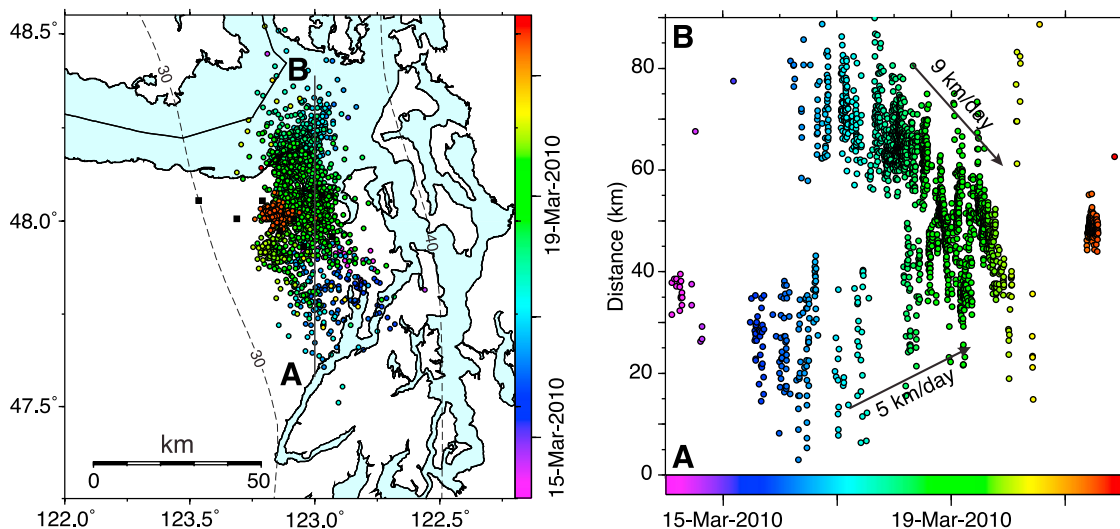

Figure 8. Evolution of a moderate-size tremor episodes occurred in March 2010, during the inter-ETS time period. Circles are tremor locations color-coded by time. (left) Map view; (right) time-distance plot. Distance is plotted along the north-south line AB drawn in the map; 2014 tremor locations are used to make this figure.

November 2009 episode
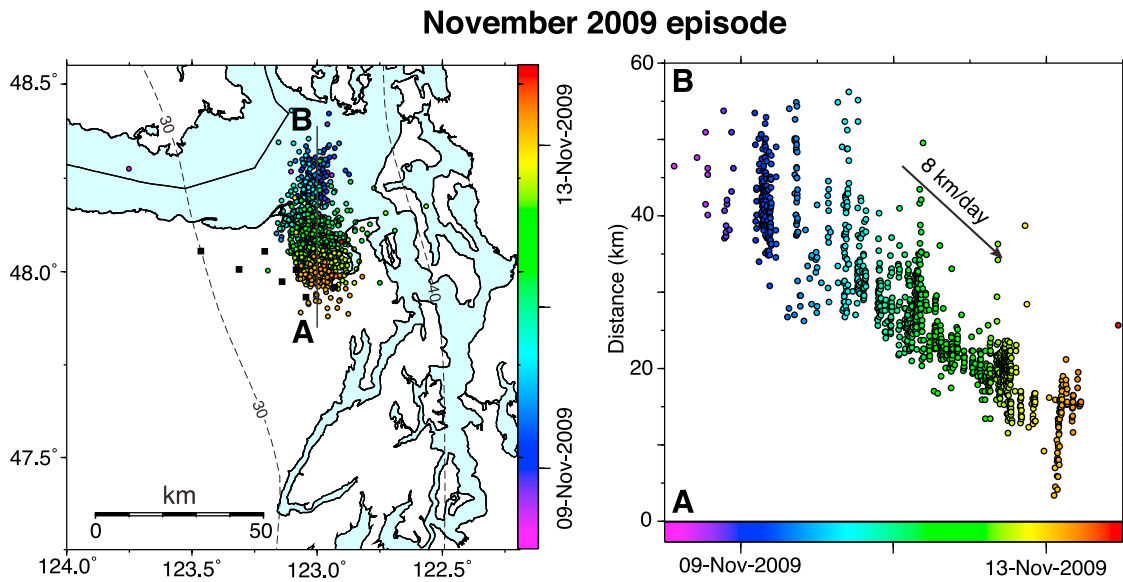
Figure 9. Evolution of a moderate-size tremor episodes occurred in November 2009, during the inter-ETS time period. Circles are tremor locations color-coded by time. (left) Map view; (right) time-distance plot. Distance is plotted along the north-south line AB drawn in the map; 1173 tremor locations are used to make this figure.

accumulation may require longer duration of tremor activity before the stress is released and rupture can propagate further, slowing down the rupture propagation velocity. In contrast, rupture propagates faster in the area between the patches possibly because of lower level of stress accumulation due to steadier aseismic slip. Hence, the patches of asperities in the transition zone likely control tremor generation and rupture propagation during slow quakes. Over shorter time-scales, evolution of slip is more complex, and may be governed by the interplay between fault plane structures, fluid pressure and stress-state.
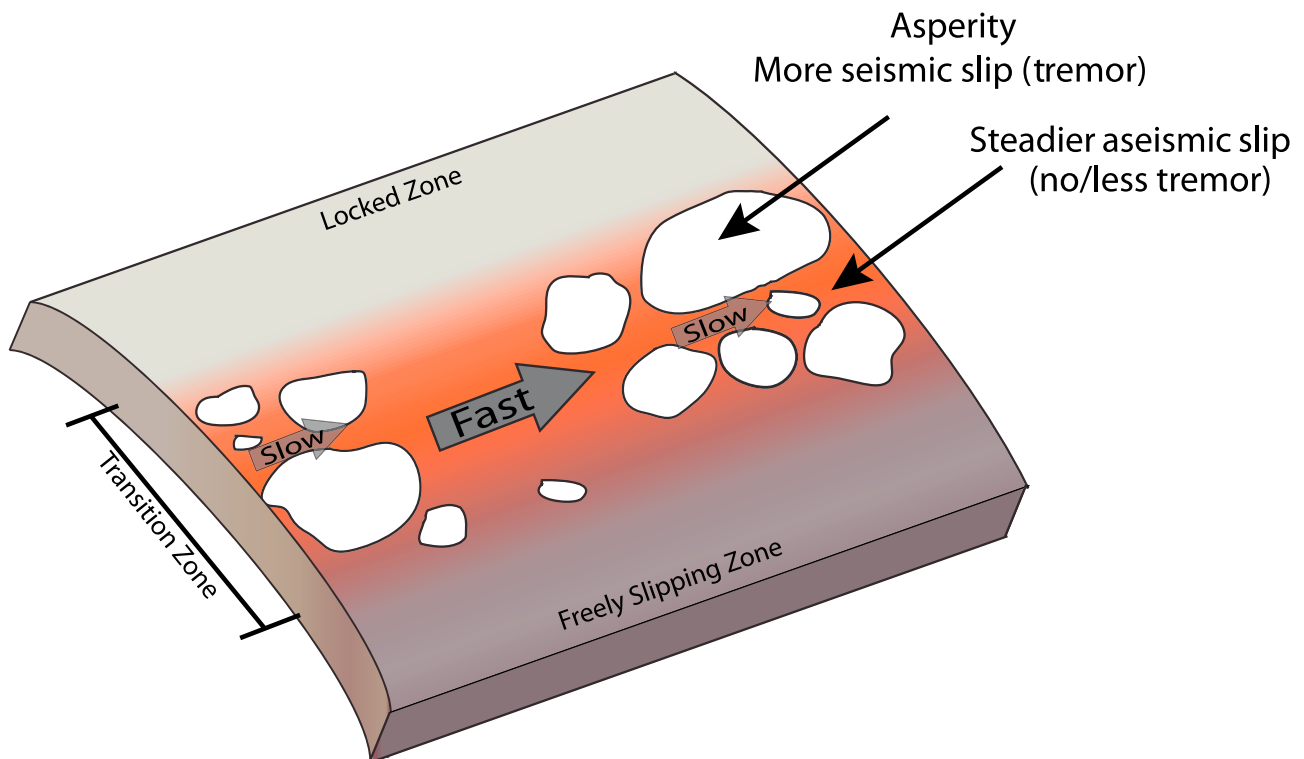
Figure 10. Schematic diagram showing a model of the transition zone.

5. Conclusions

[15] We performed a seismic experiment to image slow earthquakes using multiple mini seismic arrays. We develop a new array technique, the multibeam-backprojection method, to detect and locate tremor in high resolution. Using this technique, we show that tremor occur near the plate interface, and is likely caused by shear slip on the subduction fault. MBBP technique detects near-continuous tremor activity in Cascadia. Spatial tremor distribution is strongly heterogeneous with several patches on the fault plane producing majority of the tremor. We imaged three spatially stable downdip patches that repeatedly experience tremor episodes. Updip patches are broken only during the ETS event, but remain seismically silent during the inter-ETS time period. Successive failures of multiple patches produce major tremor episodes with coherent rupture propagation. We are able to resolve a factor of 5 variation in the velocity of along strike rupture propagation during the ETS event. The patches appear to modulate the rupture propagation velocity. Rupture propagates slowly inside the patches, and fast in between. Our observations suggest a heterogeneous transition zone with several patches that behave like asperities on the fault. The asperities, tens of kms in dimension, seem to be characterized by more seismic slip in the form of tremor relative to a more aseismically slipping background. These tremor asperities in the transition zone may control the evolution of slow earthquakes in space and time. Detailed imaging of slow earthquakes using multiple mini seismic arrays presented in this study gives new insights into the physics of enigmatic slow events, and may shed light on the factors governing seismic radiation and rupture propagation during earthquakes in general.

References

Audet, P., M. G. Bostock, D. C. Boyarko, M. R. Brudzinski, and R. M. Allen (2010), Slab morphology in the Cascadia fore arc and its relation to episodic tremor and slip, *J. Geophys. Res.*, *115*, B00A16, doi:10.1029/2008JB006053.

Crosson, R. S. (1976), Crustal structure modeling of earthquake data: 2. Velocity structure of Puget Sound region, Washington, *J. Geophys. Res.*, *81*(17), 3047–3054, doi:10.1029/JB081i017p03047.

Gerstoft, P., and T. Tanimoto (2007), A year of microseisms in southern California, *Geophys. Res. Lett.*, *34*, L20304, doi:10.1029/2007GL031091.

Ghosh, A., J. E. Vidale, Z. Peng, K. C. Creager, and H. Houston (2009a), Complex nonvolcanic tremor near Parkfield, California, triggered by the great 2004 Sumatra earthquake, *J. Geophys. Res.*, *114*, B00A15, doi:10.1029/2008JB006062.

Ghosh, A., J. E. Vidale, J. R. Sweet, K. C. Creager, and A. G. Wech (2009b), Tremor patches at Cascadia revealed by array analysis, *Geophys. Res. Lett.*, *36*, L17316, doi:10.1029/2009GL039080.

Ghosh, A., J. E. Vidale, J. R. Sweet, K. C. Creager, A. G. Wech, and H. Houston (2010a), Tremor bands sweep Cascadia, *Geophys. Res. Lett.*, *37*, L08301, doi:10.1029/2009GL042301.

Ghosh, A., J. E. Vidale, J. R. Sweet, K. C. Creager, A. G. Wech, H. Houston, and E. E. Brodsky (2010b), Rapid, continuous streaking of tremor in Cascadia, *Geochem. Geophys. Geosyst.*, *11*, Q12010, doi:10.1029/2010GC003305.

Houston, H., B. G. Delbridge, A. G. Wech, and K. C. Creager (2011), Rapid tremor reversals in Cascadia generated by a weakened plate interface, *Nat. Geosci.*, *4*(6), 404–409, doi:10.1038/ngeo1157.

Ide, S. (2010), Striations, duration, migration and tidal response in deep tremor, *Nature*, *466*(7304), 356–359, doi:10.1038/nature09251.

Ide, S., G. C. Beroza, D. R. Shelly, and T. Uchide (2007), A scaling law for slow earthquakes, *Nature*, *447*(7140), 76–79, doi:10.1038/nature05780.

Ito, Y., K. Obara, K. Shiomi, S. Sekine, and H. Hirose (2007), Slow earthquakes coincident with episodic tremors and slow slip events, *Science*, *315*(5811), 503–506, doi:10.1126/science.1134454.

Johnson, D. H., and D. E. Dudgeon (1993), *Array Signal Processing: Concepts and Techniques*, Prentice Hall, Englewood Cliffs, N. J.

Kao, H., S. J. Shan, H. Dragert, G. Rogers, J. F. Cassidy, and K. Ramachandran (2005), A wide depth distribution of seismic tremors along the northern Cascadia margin, *Nature*, *436*(7052), 841–844, doi:10.1038/nature03903.

Lay, T., H. Kanamori, and L. Ruff (1982), The asperity model and the nature of large subduction zone earthquakes, *Earthquake Predict. Res.*, *1*(1), 3–71.

McCrory, P. A., J. L. Blair, D. H. Oppenheimer, and S. R. Walter (2006), Depth to the Juan de Fuca slab beneath the Cascadia subduction margin–A 3-D model sorting earthquakes, *U.S. Geol. Surv. Data Ser.*, *91*.

Obara, K. (2002), Nonvolcanic deep tremor associated with subduction in southwest Japan, *Science*, *296*(5573), 1679–1681, doi:10.1126/science.1070378.

Obara, K. (2010), Phenomenology of deep slow earthquake family in southwest Japan: Spatiotemporal characteristics and segmentation, *J. Geophys. Res.*, *115*, B00A25, doi:10.1029/2008JB006048.

Obara, K. (2011), Characteristics and interactions between non-volcanic tremor and related slow earthquakes in the Nankai subduction zone, southwest Japan, *J. Geodyn.*, *52*(3–4), 229–248, doi:10.1016/j.jog.2011.04.002.

Obara, K., S. Tanaka, T. Maeda, and T. Matsuzawa (2010), Depth-dependent activity of non-volcanic tremor in southwest Japan, *Geophys. Res. Lett.*, *37*, L13306, doi:10.1029/2010GL043679.

Preston, L. A., K. C. Creager, R. S. Crosson, T. M. Brocher, and A. M. Trehu (2003), Intraslab earthquakes: Dehydration of the Cascadia slab, *Science*, *302*(5648), 1197–1200, doi:10.1126/science.1090751.

Rogers, G., and H. Dragert (2003), Episodic tremor and slip on the Cascadia subduction zone: The chatter of silent slip, *Science*, *300*(5627), 1942–1943, doi:10.1126/science.1084783.

Rubin, A. M., D. Gillard, and J. L. Got (1999), Streaks of microearthquakes along creeping faults, *Nature*, *400*(6745), 635–641, doi:10.1038/23196.

Rubinstein, J. L., M. La Rocca, J. E. Vidale, K. C. Creager, and A. G. Wech (2008), Tidal modulation of nonvolcanic tremor, *Science*, *319*(5860), 186–189, doi:10.1126/science.1150558.

Shelly, D. R. (2010), Periodic, chaotic, and doubled earthquake recurrence intervals on the deep San Andreas Fault, *Science*, *328*(5984), 1385–1388, doi:10.1126/science.1189741.

Shelly, D. R., G. C. Beroza, S. Ide, and S. Nakamula (2006), Low-frequency earthquakes in Shikoku, Japan, and their relationship to episodic tremor and slip, *Nature*, *442*(7099), 188–191, doi:10.1038/nature04931.

Shelly, D. R., G. C. Beroza, and S. Ide (2007), Non-volcanic tremor and low-frequency earthquake swarms, *Nature*, *446*(7133), 305–307, doi:10.1038/nature05666.

Szeliga, W., T. Melbourne, M. Santillan, and M. Miller (2008), GPS constraints on 34 slow slip events within the Cascadia subduction zone, 1997–2005, *J. Geophys. Res.*, *113*, B04404, doi:10.1029/2007JB004948.

Wech, A. G., and K. C. Creager (2008), Automated detection and location of Cascadia tremor, *Geophys. Res. Lett.*, *35*, L20302, doi:10.1029/2008GL035458.

Wessel, P., and W. H. F. Smith (1998), New improved version of generic mapping tools released, *Eos Trans. AGU*, *79*(47), 579, doi:10.1029/98EO00426.